Direct detection of evanescent electromagnetic waves at a planar dielectric surface by laser atomic spectroscopy

T. Matsudo, H. Hori, T. Inoue, H. Iwata, Y. Inoue, and T. Sakurai
Department of Electronics and Computer Science, Yamanashi University, 4-3-11 Takeda, Kofu 400, Japan
(Received 26 January 1996; revised manuscript received 2 December 1996)

The penetration depth and pseudomomentum (wave vector) of evanescent electromagnetic waves are measured at a planar dielectric surface by means of laser spectroscopy using the Cs D_2 line with a wavelength of 852.1 nm. The same experimental setup is employed in all the experiments. The first result shows a sharp, asymmetric absorption profile, which is explained in terms of the thin penetration depth, and the second shows an actual transfer of the pseudomomentum of the surface electromagnetic mode to atoms via a resonance interaction. The measured penetration depth and pseudomomentum agree with the natural interpretation of the complex wave number characterizing evanescent waves at a planar dielectric-vapor interface. Direct excitation of evanescent waves by excited Cs atoms has also been observed as atomic fluorescence emitted into the dielectric material at the angle of total internal reflection. The results are in good agreement with the theoretical predictions and exhibit the characteristics of excitation transfer or tunneling from Cs atoms into the surface mode. [S1050-2947(97)07603-8]

PACS number(s): 42.50.−p, 32.30.−r

I. INTRODUCTION

An evanescent electromagnetic (EM) wave at a planar dielectric surface is described by the classical EM theory and characterized by a complex wave number [1]

$$k_{\parallel}=k_0 n\sin\theta_i\,,$$
$$k_{\perp}=ik_0\sqrt{n^2\sin^2\theta_i-1}, \tag{1}$$

where k_0 is the wave number in vacuum, n the refractive index, and θ_i the incident angle. The natural interpretation of the complex wave number is the penetration depth ($d_{\mathrm{pen}}=|k_{\perp}|^{-1}$) in the direction normal to the boundary and the pseudomomentum ($\hbar k_{\parallel}$) parallel to the boundary associated with the translational symmetry of the material system in the direction parallel to the boundary surface. These parameters contain the problem of the light-matter (dielectric) interaction. There have been many discussions on the momentum of an EM field coupled to a material system and various controversial points have yet to be clarified [2,3] such as the Minkowski-Abraham controversy. The light-matter interaction is very complicated even in the classical or the semiclassical domain. Therefore it is useful to analyze the characteristics of evanescent waves from the microscopic viewpoint of the EM interaction of matter. In this work, we experimentally study atomic interactions with evanescent waves at a dielectric-vapor interface.

Recently, the atomic interaction with an EM field near a material surface has been of interest both in cavity quantum electrodynamics (cavity QED) [4–7] and optical near-field problems [8]. The physics common to these problems is the many-body EM interaction confined within the atom-plus-matter system in the sense that the material surface alters the boundary conditions imposed on the relevant EM interactions. Hence to clarify the nature of the evanescent wave at a planar dielectric surface is very useful not only for analysis of these problems, but also to enable progress in the fields of cavity QED and scanning near-field optical microscopy (SNOM) [9].

In the present work, we experimentally demonstrate the characteristics of the penetration depth and the pseudomomentum of the evanescent wave [10,11] by means of laser spectroscopy using the D_2 resonance line of Cs atomic vapor. We also demonstrate experimentally the reverse process in which a direct excitation of evanescent waves by excited Cs atoms takes place [12]. In all the experiments, to demonstrate the nature of evanescent waves, we use the same experimental setup in order to ensure consistency of the physical quantities measured.

II. EXPERIMENTAL SETUP

The Cs-vapor cell consists of a Pyrex glass cylinder 2 cm long with an inner diameter of 1.8 cm and a pyramidal glass prism with a right-angled apex which is attached to one end of the cylinder (Fig. 1). This allows us to excite or measure two evanescent waves propagating along orthogonal directions tangential to the Cs-vapor–glass boundary, simultaneously. The base of the prism is 2.2 cm^2, and the apex is cut off to form a 4-mm^2 flat surface in order to allow inci-

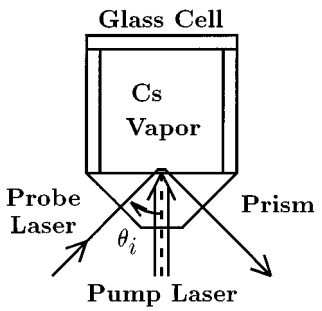

FIG. 1. Cs cell with pyramidal glass prism. The refractive index of the prism is $n\sim1.47$ around a wavelength of 852.1 nm. The critical angle of total internal reflection is $\theta_c\sim42.9°$.

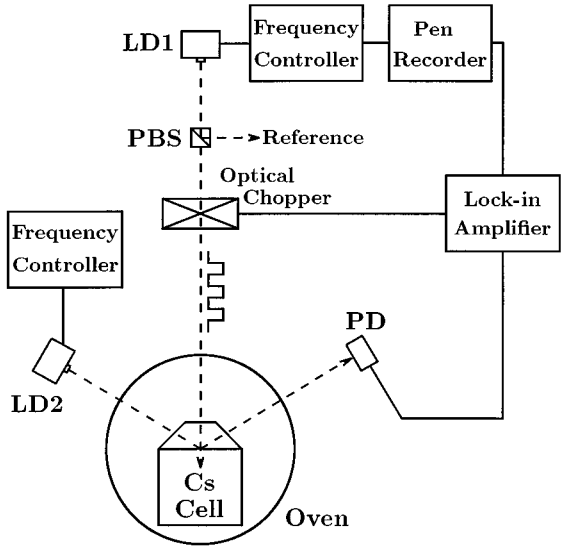

FIG. 2. Basic experimental setup for measurement of the physical characteristics of evanescent waves: LD1, pump laser; LD2, probe laser; PD, photodetector; PBS, polarizing beam splitter. This setup is especially used for measurement of the penetration depth. In other experiments, the setup is changed in some details (see text).

dence of laser beams in a direction normal to the vapor-glass interface. The refractive index of the prism is $n \sim 1.47$ for light with a wavelength of 852.1 nm, and so the critical angle for total internal reflection is $\theta_c = \sin^{-1}(1/n) \sim 42.9°$. A double thin ceramic-coated heating wire (Cerama-Wire) is wound directly onto the glass cell to control the temperature and pressure of the Cs vapor, and the current in each wire flows in an opposite direction in order to cancel the influence of the magnetic field produced by the current. The effect of the geomagnetism of about 0.3 G at our laboratory in Japan on hyperfine pumping of Cs atoms can be ignored, because the Zeeman splitting at 0.3 G is of the order of 1 kHz and much smaller than a natural linewidth of Cs atoms.

Figure 2 shows the basic experimental setup used in experiments. The light sources are frequency-controlled single-mode AlGaAs lasers (Mitsubishi Electric Corp., ML3401). The frequency of lasers is tuned to the Cs D_2 line at 852.1 nm. The energy diagram of hyperfine splitting of the Cs D_2 line is shown in Fig. 3. Precise control of the laser frequency is achieved by stabilizing the diode temperature and injection current electronically to reduce fluctuations within

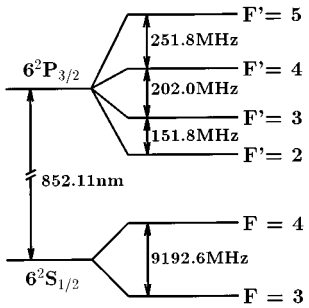

FIG. 3. Energy diagram of hyperfine splitting of the Cs D_2 line. $6\,^2S_{1/2}$ and $6\,^2P_{3/2}$ are the ground and excited states of the hyperfine energy structure, respectively.

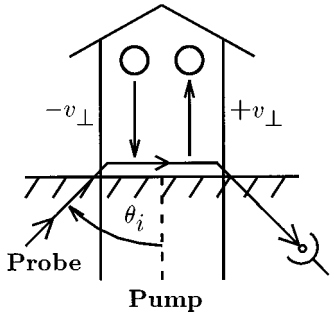

FIG. 4. Experimental scheme for the penetration depth d_{pen}. Here $v_\perp$-selected atoms are obtained by VSHP and the interaction time with the evanescent probing field determines the penetration depth.

10^{-4} K and 1 μA of the preset values, respectively. A short-term frequency excursion of the line center of the diode lasers about its mean of less than 1 MHz is maintained during the scanning time for frequencies greater than 1 GHz across the hyperfine spectrum of the excited states of the Cs D_2 line. An optical chopper is used to modulate the intensity of a pump laser at 80 Hz, and the intensity changes of a probe laser or a fluorescence induced by the pump laser is sensitively detected by a lock-in amplifier. The details of each experiment are described in following sections.

III. PENETRATION DEPTH

In this section, we treat a measurement of the penetration depth of the evanescent waves. The principle of measurement is shown in Fig. 4. One of the ground hyperfine states of Cs atoms, for example, the $6\,^2S_{1/2}\,F=4$ state, is velocity-selectively pumped with respect to $v_\perp$ using a pump laser incident normal to the glass surface from the flattened apex of the glass prism, where $v_\perp$ is the velocity component of an atom normal to the glass surface. Velocity-selective excitation described by the relation $\omega_p = \omega_0(1 + v_\perp/c)$ based on the Doppler effect clearly occurs, because both the natural linewidth of ~ 5 MHz and the laser spectral width of ~ 10 MHz are much smaller than the inhomogeneous Doppler broadening of the Cs D_2 line, which is about 400 MHz. Here ω_p is the pump frequency, ω_0 is the resonance frequency of the Cs D_2 line, for example, from the $6\,^2S_{1/2}\,F=4$ state to the $6\,^2P_{3/2}\,F'=3$ state, and c is the velocity of light. Velocity-selective excited atoms in the $6\,^2P_{3/2}\,F'=3$ state decay into the ground hyperfine states, the $6\,^2S_{1/2}\,F=3$ and $F=4$ states. Repeating such a cycle, atoms are velocity-selectively pumped from the $6\,^2S_{1/2}\,F=4$ of ground state to the $6\,^2S_{1/2}\,F=3$ state. This technique is referred to as velocity-selective hyperfine pumping (VSHP). The velocity-selectively pumped atoms in one ground state interact with the frequency-locked evanescent probing field, and the resulting intensity change in the probe laser due to the absorption by the velocity-selective pumped atoms is measured as a function of pump frequency. Since the wave vector of the pump laser is orthogonal to that of the probe laser, the spectrum of the pumped atom is seen by the probe laser as the Gaussian velocity distribution. Therefore the probe laser may be tuned to anywhere in the Doppler-broadened absorption line.

The spectral profile $\alpha(\omega_p,\omega_s)$ given by the probe absorption due to the pumped atom as a function of the pump frequency ω_p and the probe frequency ω_s is written as

$$\alpha(\omega_p,\omega_s)=\sigma_s\int_{-\infty}^{+\infty}dv_\parallel\int_{-\infty}^{+\infty}dv_\perp\rho(v_\perp)\times L_p(\omega_p,v_\perp)\xi_s(\omega_s,v_\parallel,v_\perp)W(v_\parallel,v_\perp), \quad (2)$$

$$\rho(v_\perp)=N\frac{\gamma_N}{\gamma_N+|k_\perp||v_\perp|}, \quad (3)$$

$$L_p(\omega_p,v_\perp)=\frac{1}{\pi}\frac{\gamma_N}{(\omega_p-\omega_0+k_0v_\perp)^2+\gamma_N^2}, \quad (4)$$

$$\xi_s(\omega_s,v_\parallel,v_\perp)=\frac{1}{\pi}\frac{\gamma_N+|k_\perp||v_\perp|}{(\omega_s-\omega_0+k_\parallel v_\parallel)^2+(\gamma_N+|k_\perp||v_\perp|)^2}, \quad (5)$$

$$W(v_\parallel,v_\perp)=\frac{1}{\pi u^2}\exp\left(-\frac{v_\parallel^2+v_\perp^2}{u^2}\right), \quad (6)$$

where $k_0=\omega_0/c$, u is the average thermal velocity, μ is the electric dipole moment, $\sigma_s=\pi|\mu|^2\omega_s/3\varepsilon_0\hbar c$ is the absorption cross section of the probe laser at the center of the resonance ε_0 is the dielectric constant in vacuum, and $2\gamma_N$ is the effective absorption linewidth, which is the sum of the natural width of the Cs D_2 line, 5 MHz, and the linewidth of the pump laser, 10 MHz. Here $\rho(v_\perp)$ is the number of pumped atoms measured by the evanescent probe laser, $L_p(\omega_p,v_\perp)$ is the normalized spectral line shape of the pumped atom, and $\xi_s(\omega_s,v_\parallel,v_\perp)$ is the normalized spectral line shape of atoms interacting with the thin evanescent probe laser. The power broadening of both line shapes due to the pump and probe lasers is ignored because the width does not influence the profile of $\alpha(\omega_p,\omega_s)$ under the experimental condition. $W(v_\parallel,v_\perp)$ represents the Gaussian velocity distribution of the atoms.

The quantity N in Eq. (3) is proportional to the excess population of velocity selective pumped atoms in the relevant ground hyperfine state in the interaction region with the evanescent probing field and depends strongly on the sign of the pump detuning, $\Delta\omega_p=\omega_p-\omega_0$. Atoms with $v_\perp$ approaching the surface ($v_\perp<0$) interact with the red-detuned propagating pumping field. Then a significant population difference due to VSHP is steadily established between the ground hyperfine states before the selected atoms interact with the evanescent probing field. For $v_\perp\leqslant 0$ at red detuning ($\Delta\omega_p<0$), N is considered to be constant since the VSHP saturates the population difference in the steady state. When the pump frequency is blue detuned, atoms with $v_\perp$ departing from the surface ($v_\perp>0$) leave the evanescent probing field within a typical pumping time of ~ 1 μs, which is the time required to establish the saturation of a population difference in the VSHP process when the pump intensity is ~ 1 mW/cm^2, which is typical to the present experiments. For $v_\perp>0$ at blue detuning ($\Delta\omega_p>0$), N can be approximated to zero, since atoms leave the evanescent region even with insufficient pumping. Therefore the difference between the red-detuning and blue-detuning pumping conditions results in the asymmetry of the signal.

Next, we consider the interaction between the evanescent probe laser and the hyperfine pumped atoms of the density N at red detuning ($\Delta\omega_p<0$) of the pump frequency. Atoms with $|v_\perp|\leqslant d_{\rm pen}/\tau_{\rm sp}$ interact with the evanescent probing field over the period required to maintain the natural linewidth in the absorption signal. Here $\tau_{\rm sp}$ is the spontaneous lifetime of the atom and $d_{\rm pen}$ is the penetration depth. This relationship is valid for relatively small red detuning of the pump frequency. Atoms with $|v_\perp|>d_{\rm pen}/\tau_{\rm sp}$ are considered to have a decay constant due to a relatively short transit time $\tau_{\rm tr}=(|k_\perp||v_\perp|)^{-1}$, and the number of atoms interacting with the probe laser decreases by the factor $\gamma_N/(\gamma_N+|k_\perp||v_\perp|)$. The actual density of the atom measured by the probe laser is given by $N\gamma_N/(\gamma_N+|k_\perp||v_\perp|)$ as shown in Eq. (3). This is true for relatively large red detuning of the pump frequency and has a close relationship to the sharpness and asymmetry of the spectrum with respect to the resonance frequency ω_0 of the pump laser.

In Eq. (5), the width of the normalized Lorentzian $\xi_s(\omega_s,v_\parallel,v_\perp)$ is broadened by the effective linewidth and the transit effect due to interaction with the thin evanescent probing field, and the width depends on the velocity $v_\perp$. When atoms with velocity $v_\perp$ cross the evanescent field, which decays exponentially with decay constant $|k_\perp|$, the accurate spectral shape due to the transit effect may be slightly different from pure Lorentzian; however, as the first-order approximation, we here assume the shape as Lorentzian with a width of $\Delta\omega=\gamma_N+|k_\perp||v_\perp|$, i.e., the sum of the effective linewidth and the transit width.

In order to evaluate the effect of penetration depth on the observed spectrum in the red-detuning region, it is informative to use an approximated form of $\alpha(\omega_p,\omega_s)$ due to the Doppler limit approximation, $\gamma_N+|k_\perp||v_\perp|\ll w_D$ ($=k_0u\sqrt{\ln 2}$, half of the Doppler width)

$$\alpha(\omega_p,\omega_s)\sim C_s\left(1+\frac{1}{\gamma_N\omega_0}\frac{\Delta\omega_p}{d_{\rm pen}/c}\right)^{-1} \quad (\text{at } \Delta\omega_p<0 \text{ and } |\Delta\omega_p|\ll w_D), \quad (7)$$

where $C_s=\sigma_sN\ln 2/(\pi w_{Dp}w_{Ds})$ is constant and $w_{Dp}=w_D$ and $w_{Ds}=w_Dn\sin\theta_i$ are the Doppler widths in relation to atoms with $v_\perp$ and $v_\parallel$, respectively. Therefore the penetration depth $d_{\rm pen}$ can be calculated from the gradient of the inverse of $\alpha(\omega_p,\omega_s)$ with respect to red detuning, $\Delta\omega_p<0$ around the line center. For blue-detuned pump frequencies, the interaction process is limited by the pumping time and $\rho(v_\perp)$ is close to zero as mentioned previously. Therefore the spectral width is given by γ_N, and the sharp edge shows the usual Doppler-free spectrum at $\Delta\omega_p>0$. Thus the overall spectral profile depends on the pump detuning with respect to the atomic resonance frequency ω_0.

In the experiment shown in Fig. 2, a relatively high cell temperature of up to 410 K results in a Cs-vapor density of $N_0\sim 1\times 10^{14}$ cm^{-3}, which is necessary for absorption measurements using evanescent waves with very small penetration depths. The propagating pump beam, which has a power of 500 μW and a diameter of 2 mm, is incident normal to the glass-vapor interface. The frequency-locked probe laser,

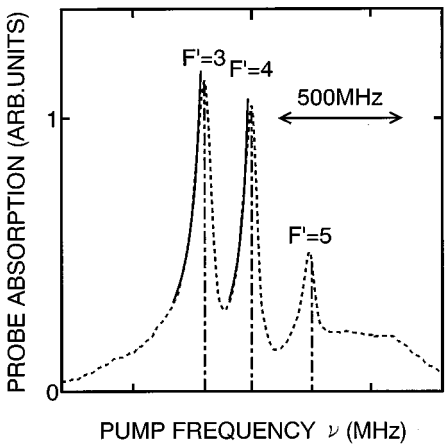

FIG. 5. Probe absorption versus pump frequency of the Cs D_2 line ($6\,^2S_{1/2}\ F=4 \rightarrow 6\,^2P_{3/2}$). The probe frequency is locked at the transition from $6\,^2S_{1/2}\ F=3$. The dashed line shows the observed spectrum including the hyperfine components $F'=3$, 4, and 5. The solid lines show the red wing slope estimated theoretically in the near-resonance regime. Incident angles of the pump and probe lasers are $\theta_{\text{pump}}=0°$ and $\theta_{\text{probe}}=47°$, respectively.

which has a power of 100 μW and a diameter of 2 mm, is incident at an angle of total internal reflection, $\theta_i \sim 47°$, which is slightly larger than the critical angle 42.9°. The corresponding penetration depth of the evanescent wave is $d_{\text{pen}}=0.34\ \mu$m. The averaging time for lock-in detection is 1 s, and the sweeping rate of the laser frequency is about 200 MHz/min with an accuracy less than the natural linewidth. The experimental scheme is shown in Fig. 4. The signal due to absorption of the evanescent probing field by the $v_\perp$-selected atoms is recorded as a function of the pump detuning.

Figure 5 shows a spectrum measured using a pump frequency swept through three hyperfine transitions from $6\,^2S_{1/2}\ F=4$ to $6\,^2P_{3/2}\ F'=3$, 4, and 5 and a probe frequency locked to the peak transition from the pumped ground hyperfine state $6\,^2S_{1/2}\ F=3$ to the excited state $6\,^2P_{3/2}$. Since the hyperfine splitting in three excited states of $6\,^2P_{3/2}$ is less than the Doppler width, the frequency-locked probe laser is resonant simultaneously with the upper hyperfine states $F'=2$, 3, and 4. The spectra as a function of the frequency of the pump laser shown in Fig. 5 are clearly separated in three sharp hyperfine components of $6\,^2P_{3/2}$ state and asymmetrical with respect to the resonance frequencies corresponding to the transitions to the $6\,^2P_{3/2}$ $F'=3$ and 4 states, even though the axis of the pump laser is perpendicular to that of the probe laser. Here the evanescent probing field is p polarized (TM mode). The spectral profile measured using an s-polarized (TE-mode) probe is the same as that for the p-polarized probe. In addition, the experimental result for sweeping the probe frequency ω_s shows the usual Doppler profile when the pump frequency ω_p is locked, for example, at the peak of the transition from the $6\,^2S_{1/2}\ F=4$ to the $6\,^2P_{3/2}\ F'=3$ and agrees with Eq. (2).

The slopes indicated by the solid lines in Fig. 5 show theoretically predicted values in the near-resonance regime calculated using Eq. (7) for the penetration depth of $d_{\text{pen}}=0.34\ \mu$m under the conditions used in this experiment. The results are in good agreement with the experimental profile. The penetration depth d_{pen} can be estimated from the shape of the spectrum obtained with red detuning, $\Delta\omega_p<0$. The broad background seen in Fig. 5 might be due to velocity mixing of the pumped atoms due to collisions at the prism surface. The pumped atoms still maintain a population difference in the ground state.

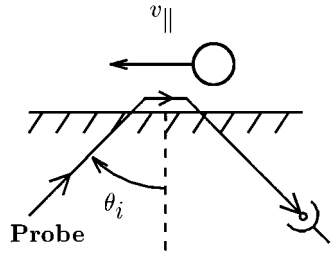

FIG. 6. Experimental scheme for the pseudomomentum. The Doppler broadening of absorption profile is observed using an evanescent wave probe laser. The pseudomomentum is estimated from the spectral width and is larger than the photon momentum is vacuum.

It is remarkable that in Fig. 5 the Doppler-free spectrum in the probe laser resonating with the $6\,^2S_{1/2}\ F=3$ is also observed at the pump resonance frequency from the $6\,^2S_{1/2}$ $F=4$ to the $6\,^2P_{3/2}\ F'=5$. The existence of this Doppler free spectrum at the transition from $F=4$ to $F'=5$ cannot explain from the consideration of a dipole transition, because the spontaneous transition from the $F'=5$ to the $6\,^2S_{1/2}$ $F=3$ is forbidden due to the selection rule $\Delta F=0,\pm 1$, and the hyperfine pumping to $F=3$ does not occur by using the pump laser at the resonance frequency from $F=4$ to $F'=5$ in VSHP experiments. Mixing of the excited hyperfine states in the $6\,^2P_{3/2}$ state is one possible cause of this anomalous VSHP resonance. An extensive study, both experimental and theoretical, should be carried out to account for this phenomenon as a characteristic of atomic interactions with the optical near field. This experimental technique can be used not only for measurement of the penetration depth, but also to investigate atom-surface interactions [13,14].

IV. PSEUDOMOMENTUM

As stated in the Introduction, an evanescent wave results from coupling of an EM field with a material system at a planar dielectric interface. Because of the discontinuity at the interface, the spatial translational symmetry of the system is restricted. This results in a complex wave number, and the real part corresponds to the pseudomomentum or wave vector, which is a conserved quantity under parallel displacement of the system. Both the EM and material momentum contribute to the pseudomomentum, the magnitude of which is larger than that of the EM momentum in vacuum at the same frequency. It is therefore useful to demonstrate the role of the pseudomomentum as a conserved quantity in resonant interactions between atoms and evanescent waves, in which the energy transfer from the EM field to atoms is governed by a quantum transition in the atomic states.

The principle of measurement is shown in Fig. 6. In experiments, the Doppler shift of the atomic resonance is closely related to the pseudomomentum. The Doppler shift is

explained on an atomic scale as compensation for the change in kinetic energy of atoms due to momentum transfer associated with photon absorption. In the case of photon absorption in vacuum, the momentum of the atom-plus-photon system should be conserved, and so the Doppler shift of the atomic resonance is equal to the photon momentum times the atomic velocity divided by Planck's constant, i.e., $[(\hbar\omega_0/c)v]/\hbar=\omega_0 v/c$. In contrast, in the case of atomic interactions with evanescent waves, the conserved quantity is the pseudomomentum of the system, so that when a photon with energy $\hbar\omega_0$ is absorbed, the associated momentum transfer is $\hbar k_\parallel$, which is larger than $\hbar\omega_0/c$. The excess momentum transfer is from the dielectric. An atom is a simple microscopic system, and so the pseudomomentum of a many-body system is transferred at the surface to atoms as a real momentum. Therefore the demonstration of pseudomomentum conservation in resonant absorption also gives an indication of the dynamical effect of an optical near field on atoms. If the pseudomomentum is conserved in the atomic interaction with evanescent waves at total internal reflection, then the Doppler shift $\Delta\omega_D$ of the atomic resonance frequency is proportional to the real part of the complex wave number $k_\parallel$ as

$$\Delta\omega_D=\pm k_\parallel v_\parallel=\pm\frac{\omega_0}{c}v_\parallel n\sin\theta_i, \tag{8}$$

where θ_i is the angle of the incident plane wave. The Doppler shift is observed simply as inhomogeneous broadening or Doppler broadening of the atomic absorption line due to the thermal velocity distribution along the wave vector of the evanescent wave. The spectral profile of a single absorption line is given by [11,15,16]

$$\alpha(\omega_s)=N_0\sigma_s\int_{-\infty}^{+\infty}dv_\parallel\int_{-\infty}^{+\infty}dv_\perp\xi_s(\omega_s,v_\parallel,v_\perp)W(v_\parallel,v_\perp), \tag{9}$$

where the Lorentzian $\xi_s(\omega_s,v_\parallel,v_\perp)$ and Gaussian $W(v_\parallel,v_\perp)$ profiles and the absorption cross section σ_s are those in Eq. (2), and N_0 is the density of Cs atomic vapor. In Eq. (9), the Lorentzian broadening due to the transit effect for atoms with nonzero $v_\perp$ is taken into account as shown in Eq. (5). The absorption signal of the Cs D_2 line actually consists of three Doppler-broadened hyperfine spectra.

The whole experimental setup is the same as that shown in Fig. 2 except for removing the pump laser, the chopper, and the lock-in amplifier. A p-polarized diode laser beam with an intensity of $\sim$100 μW and a diameter of 2 mm is incident at an angle of total internal reflection, θ_i. The intensity change due to absorption of the reflected probe beam is measured for frequencies swept through the Doppler-broadened absorption spectrum of the Cs D_2 line from the $6\,^2S_{1/2}\ F=3$. The full width at half maximum (FWHM) of the Doppler-broadened absorption spectrum is measured as a function of θ_i, which is larger than the critical angle θ_c. Both the signal-to-noise ratio and the reproducibility of the observed spectrum are sufficient to discuss the enhancement of the Doppler broadening with an accuracy of $\sim$10 MHz. We simultaneously use a setup for saturated absorption spectroscopy of the Cs D_2 line in order to monitor the accuracy of the swept frequency.

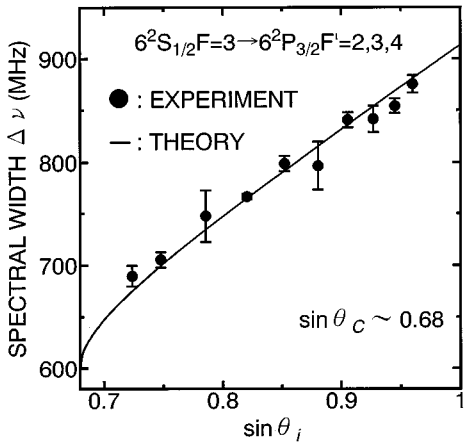

FIG. 7. FWHM of the Doppler-broadened absorption profile of the Cs D_2 line ($6\,^2S_{1/2}\,F=3\rightarrow6\,^2P_{3/2}$) as a function of the incident angle θ_i of the probe laser. The solid curve indicates the theoretical curve.

The results of the FWHM are shown in Fig. 7. The enhancement of the Doppler width due to the near-field effect is dependent on the incident angle θ_i. The FWHM of the line profile calculated using Eq. (9) taking account of the three hyperfine components is shown by the solid line in Fig. 7. The measured spectral width is in good agreement with the theoretical curve. This point is relevant to the Minkowski-Abraham controversy regarding the momentum of the EM field in a material medium of refractive index n [2,17,18]. According to the formulation by Minkowski, the momentum is nE/c; in contrast, Abraham's result is E/nc, where E is the energy of the light. The result obtained here shows not the photon momentum transfer $\hbar\omega_0/c$, but the pseudomomentum transfer $(\hbar\omega_0/c)n\sin\theta_i$ due to the atomic absorption of a photon from evanescent waves. The experimental fact that the pseudomomentum is transferred to the atom in the EM interaction near the material surface may be consistent with the Minkowski's result.

In addition to the present experiments, we have demonstrated the pseudomomentum transfer using a spectral hole burning technique and saturated absorption spectroscopy, in which counterpropagating evanescent waves with different wave numbers are used as the pumping and probing fields. The results indicate splitting of the crossover resonance according to the difference between the wave numbers of the pumping and probing fields. These results will be published elsewhere [19]. From the experimental results, it is concluded that the pseudomomentum is conserved in atomic interactions with evanescent waves and that its magnitude is related to the penetration depth.

V. DIRECT EXCITATION OF EVANESCENT WAVES

In this section we report the observation of direct excitation of evanescent waves by excited atoms, i.e., photon emission from excited atoms into the evanescent mode of a dielectric surface. This is the reverse of the absorption process. The principle of measurement is shown in Fig. 8. According to Fresnel's formula and Snell's law, a light wave traveling from a dielectric medium of refractive index n_1 can be trans-

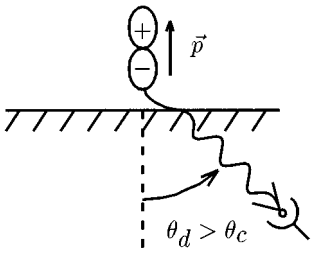

FIG. 8. Experimental scheme for the direct excitation of evanescent waves. Spontaneous radiation from an atomic dipole $\vec{p}$ excited in the direction normal to the dielectric surface is observed at the angle of total internal reflection in order to measure the direct excitation of evanescent waves. $\vec{p}$ indicates a vector atomic dipole.

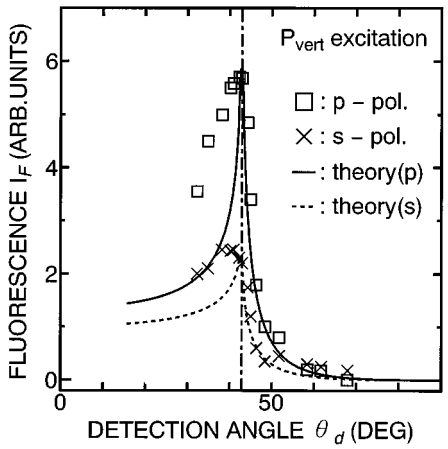

FIG. 9. Maximum intensity at the central frequency of the fluorescence excitation spectrum as a function of the detection angle θ_d. Here P_{vert} excitation indicates that the atomic dipole is excited by an electric field polarized in the direction normal to the dielectric surface.

mitted to a medium of refractive index n_2 higher than n_1 only at an angle less than the critical angle of total internal reflection. This is not the case for light emission from an excited atom in the optical near-field regime, in which the interaction of atomic dipoles with the dielectric interface affects the energy transfer.

The whole experimental setup is the same as that used for the pseudomomentum measurements except for the addition of a photodetector used to observe the spontaneous emission passing through the prism in the direction orthogonal to the evanescent waves. The cell temperature of 305 K results in a Cs vapor density of $N_0 \sim 1 \times 10^{11}$ cm^{-3}. An exciting laser beam with a power of 500 μW and a diameter of 2 mm is incident on the glass prism of the Cs cell at a total internal reflection angle of $\theta_i \sim 50°$ and tuned to the transition from the ground sate of $6\,^2S_{1/2}$ $F=3$ to the excited state of $6\,^2P_{3/2}$. The corresponding penetration depth is ~ 0.26 μm. Atoms with $v_\perp \sim 0$ are also selectively excited because the absorption spectrum for atoms with large $v_\perp$ is broadened significantly due to the short interaction duration with the thin evanescent exciting field. The spontaneous radiation from Cs atoms in the $6\,^2P_{3/2}$ state excited by the interaction with evanescent waves is detected using a photomultiplier on the dielectric side. The radiation emerges from the facet in the direction orthogonal to the laser incident facet of the pyramidal prism via direction selector apertures, each of which consists of two slits 1 mm wide, separated by a distance of 25 cm, and provides a geometrical angular resolution of $\sim \pm 0.5°$. The emission intensity is measured as a function of the angle of detection in the plane perpendicular to the incident plane of the exciting laser beam.

The maximum intensity at the central frequency of the fluorescence excitation spectrum is plotted in Fig. 9 as a function of the detection angle, which is varied around the critical angle of total internal reflection. The radiation patterns are observed for both p(TM)- and s(TE)-polarized fluorescence. Each point of data shown in Fig. 9 is an average of the measured intensity. Experimental data obtained in repeated experiments scatter about 10% around each data and the error is mainly caused by an uncertainty of the geometrical angle of detection. As seen in Fig. 9, the spontaneous radiation from Cs atom is observed even for detection angles greater than the critical angle of total internal reflection, $\theta_d > \theta_c \sim 42.9°$. Thus the direct excitation of evanescent waves, which is the reverse process of absorption, is demonstrated. The results can be interpreted in several ways, including the interaction of excited atoms with evanescent waves (both classical and quantum), the interaction between excited atoms and image dipoles, which is usually used in cavity-QED treatments, or the many-body interaction of atoms with surface polarizations.

We theoretically calculate the angular distribution of the spontaneous radiation from an oscillating dipole near a dielectric surface by using the calculations described by Carniglia *et al.* [20,21] and Burgmans *et al.* [22], assuming that atomic dipoles are initially excited in the direction vertical to the dielectric surface by the exciting evanescent wave of the TM-mode incidence. Carniglia *et al.* have calculated the angular distribution from the quantization of the evanescent wave, and Burgmans *et al.* also have calculated it by using the angular spectrum representation of a dipole field. Their results indicate the same angular dependence of the fluorescence intensity. The calculated results [23] are also shown in Fig. 9 by a solid line for p polarization of the fluorescence and a dashed line for s polarization. In the calculation, we take account of the hyperfine coupling due to the fact that the optical transitions in atomic Cs take place between hyperfine states, in which the atomic orbital angular momentum couples with the electron and nuclear spins due to internal magnetic interactions, and also assume that average atomic dipoles lie at the position of the penetration depth of the excitating evanescent wave from the surface (~ 0.26 μm). In the figure, the peaks of theoretical curves are fitted to the experimental data at θ_c. The calculated results are almost in good qualitative agreement with the experimental results, for both p and s polarizations, at $\theta_d \geqslant \theta_c$. The difference between experimental data and theoretical curves at $\theta_d < \theta_c$ may be due to two reasons. First, atoms absorbing the original spontaneous emission reemit the photon at the position out of the penetration depth and the reemitted photons can be added at the position out of the penetration depth and the reemitted photons can be added to the original signal at $\theta_d < \theta_c$. The reemitted photons out of the evanescent mode cannot observed at $\theta_d > \theta_c$. Second, atomic dipoles are initially excited in the direction not only vertical, but also parallel to the dielectric surface because the actual polariza-

tion of the EM field of the exciting evanescent wave has the component of the polarization not only vertical, but also parallel to the surface. The existence of the parallel component of atomic dipoles enhances mainly the radiation at $\theta_d < \theta_c$ [1,20–23]. However, these effects are not included in the calculation, since we are mainly interested in the excitation of evanescent waves at $\theta_d > \theta_c$.

Burgmans *et al.* investigated a transient excitation process in which atoms depart from a glass surface under excitation by propagating laser light at normal incidence [22]. In terms of a generalized cavity-QED concept, this corresponds to the modified spontaneous emission from atoms near a boundary surface or material system. The modification of the EM interaction due to the dielectric surface makes it possible for atoms to radiate into evanescent mode of the dielectric surface. This remarkable phenomenon has been effectively used to investigate atomic or molecular interactions with surfaces, such as the emission [20] and Raman scattering [24,25] from molecules at a dielectric surface and the van der Waals and Casimir-Polder forces exerted on atoms [13,14].

VI. CONCLUSION

We have demonstrated experimentally the physical characteristics and consistency of the penetration depth and pseudomomentum of an evanescent EM field at total internal reflection by means of resonance interaction measurements of the Cs D_2 line. The penetration depth affects the narrowing of the absorption spectrum due to the transit effect of atoms approaching a dielectric surface. The pseudomomentum is measured as a large Doppler broadening of the absorption line of atoms traveling in a direction parallel to the surface, and the magnitude of the pseudomomentum may be consistent with the Minkowski's result. The results are in good agreement with those calculated based on an interpretation of the complex wave number characterizing evanescent waves; i.e., the real part is related to the pseudomomentum and the imaginary part is related to the inverse of the penetration depth. The techniques developed in the present work provide a useful basis both for further investigation of atomic interactions in optical near fields and for manipulation and control of atomic states and motion using a confined EM field.

It would also be interesting to demonstrate the penetration depth and pseudomomentum for a general configuration of the optical near-field interaction of atoms in terms of the angular spectrum representation [26]. For example, the pseudomomentum becomes very large at a highly corrugated dielectric surface, and therefore significant enhancement of the Doppler shift and the associated atomic recoil occurs.

We have also demonstrated the direct excitation of evanescent waves by atoms in the excited state as spontaneous radiation at the angle of total internal reflection. We discussed the excitation transfer or tunneling features related to this phenomenon. A study of these characteristics from the viewpoint of the atomic radiation characteristics is a cavity-QED problem. These characteristics are much more pronounced when the material surface exhibits resonance characteristics, and optical near-field interaction problems then involve physics related to materials of subwavelength size [8].

ACKNOWLEDGMENTS

The authors would like to thank M. Yamaguchi for technical assistance and Dr. T. Yabuzaki and Dr. M. Kitano for stimulating comments and discussions. This work was partly supported by a Grant-in-Aid for Scientific Research from the Ministry of Education, Science, Sports and Culture.

[1] M. Born and E. Wolf, *Principles of Optics*, 5th ed. (Pergamon Press, New York, 1975).
[2] D. F. Nelson, Phys. Rev. A **44**, 3985 (1991).
[3] M. Kristensen and J. P. Woerdman, Phys. Rev. Lett. **72**, 2171 (1994).
[4] V. Sandoghdar, C. I. Sukenik, and E. A. Hinds, Phys. Rev. Lett. **68**, 3432 (1992).
[5] D. Meschede, W. Jhe, and E. A. Hinds, Phys. Rev. Lett. **41**, 1587 (1990).
[6] W. Jhe and J. W. Kim, Phys. Rev. A **51**, 1150 (1995).
[7] M. Janowicz and W. Żakowicz, Phys. Rev. A **50**, 4350 (1994).
[8] H. Hori, in *Near Field Optics*, edited by D. W. Pohl and D. Courjon (Kluwer Academic, Dordrecht, 1993), p. 105.
[9] For a recent overview of SNOM and related techniques, see Ref. [8], and also the special issue of Ultramicroscopy **57** (February 1995).
[10] S. Huard and C. Imbert, Opt. Commun. **24**, 185 (1978).
[11] G. Nienhuis, F. Schuller, and M. Ducloy, Phys. Rev. A **38**, 5197 (1988).
[12] T. Matsudo *et al.*, Technical Digest of the Pacific Rim Conference on Laser and Electro-Optics, Chiba, 1995 (unpublished), pp. 201–202.
[13] M. Chevrollier *et al.*, J. Phys. (France) II **2**, 631 (1992).
[14] M. Fichet *et al.*, Phys. Rev. A **51**, 1553 (1995).
[15] P. Boissel and F. Kerherve, Opt. Commun. **37**, 397 (1981).
[16] E. Pfleghaar, A. Marseille, and A. Weis, Phys. Rev. Lett. **70**, 2281 (1993).
[17] R. Peierls, *More Surprises in Theoretical Physics* (Princeton University Press, Princeton, 1991), Sec. 2.
[18] J. P. Gordon, Phys. Rev. A **8**, 14 (1973).
[19] T. Matsudo *et al.* (unpublished).
[20] C. K. Carniglia, L. Mandel, and K. H. Drexhauge, J. Opt. Soc. Am. **62**, 479 (1972).
[21] C. K. Carniglia and L. Mandel, Phys. Rev. D **3**, 280 (1971).
[22] A. L. J. Burgmans, M. F. H. Schuurmans, and B. Bolger, Phys. Rev. A **16**, 2002 (1977).
[23] T. Inoue *et al.* (unpublished).
[24] J. M. Vigoureux and R. Payen, J. Phys. (Paris) **36**, 1327 (1975).
[25] A. M. Steinberg and R. Y. Chiao, Phys. Rev. A **49**, 3283 (1994).
[26] E. Wolf and M. Nieto-Vesperinas, J. Opt. Soc. Am. A **2**, 886 (1985).